Coherent digital demodulation of single-camera *N*-projections for 3D-object shape measurement: Co-phased profilometry

M. Servin,[1,*] G. Garnica,[1] J. C. Estrada,[1] and A. Quiroga[2]

[1]*Centro de Investigaciones en Optica A. C., Loma del Bosque 115, 37150 Leon Guanajuato, Mexico*
[2]*Optics Department, Universidad Complutense de Madrid, Facultad de Ciencias Fisicas, Ciudad Universitaria s/n, 28040 Madrid, Spain*
[*]*mservin@cio.mx*

Abstract: Fringe projection profilometry is a well-known technique to digitize 3-dimensional (3D) objects and it is widely used in robotic vision and industrial inspection. Probably the single most important problem in single-camera, single-projection profilometry are the shadows and specular reflections generated by the 3D object under analysis. Here a single-camera along with *N*-fringe-projections is (digital) coherent demodulated in a single-step, solving the shadows and specular reflections problem. Co-phased profilometry coherently phase-demodulates a whole set of *N*-fringe-pattern perspectives in a single demodulation and unwrapping process. The mathematical theory behind digital co-phasing *N*-fringe-patterns is mathematically similar to co-phasing a segmented *N*-mirror telescope.

OCIS codes: (120.0120) Instrumentation, measurement, and metrology; (120.5050) Phase measurement; (120.4630) Optical inspection.

References and links

1. K. J. Gasvik, *Optical Metrology*, 3rd ed. (John Wiley & Sons, 2002).
2. D. Malacara, M. Servin, and Z. Malacara, *Interferogram Analysis for Optical Testing*, 2nd ed. (CRC Taylor & Francis, 2005).
3. S. S. Gorthi and P. Rastogi, "Fringe projection techniques: Wither we are?" Opt. Lasers Eng. **48**(2), 133–140 (2010).
4. Z. Wang, D. A. Nguyen, and J. C. Barnes, "Some practical considerations in fringe projection profilometry," Opt. Lasers Eng. **48**(2), 218–225 (2010).
5. W. H. Su, C. Y. Kuo, C. C. Wang, and C. F. Tu, "Projected fringe profilometry with multiple measurements to form an entire shape," Opt. Express **16**(6), 4069–4077 (2008).
6. X. Liu, X. Peng, H. Chen, D. He, and B. Z. Gao, "Strategy for automatic and complete three-dimensional optical digitization," Opt. Lett. **37**(15), 3126–3128 (2012).
7. S. Lee and L. Q. Bui, "Accurate estimation of the boundary of a structured light pattern," J. Opt. Soc. Am. A **28**(6), 954–961 (2011).
8. R. Gannavarpu and P. Rastogi, "Fringe analysis: premise and perspectives," Opt. Lasers Eng. **50**(8), iii–x (2012).
9. M. Servin, J. C. Estrada, and J. A. Quiroga, "The general theory of phase shifting algorithms," Opt. Express **17**(24), 21867–21881 (2009).

1. Introduction

Digital fringe projection 3D profilometry continues to be an active research field as can be seen from the references on this paper [1–9]. In 2010 Gorthi and Rastogi [3] review the major techniques used in 3D shape measurement. Also Wang et al. [4] published practical considerations to take into account when measuring 3D shapes using digital profilometry. Su et al. [5], and Liu et al. [6] explore how to integrate *N*-camera-projector systems which generates *N*-fringe-patterns from different positions to obtain a single 3D shape measurement.

In previous non-coherent integration of *N*-camera-projector profilometry systems, one must first estimate the fringe-boundaries of the *N*-digitized fringe-patterns [3–7]. This *N*-times fringe-boundary estimation is followed by *N*-phase-demodulations, which in turn is followed by *N*-phase-unwrappings. Doing *N*-times this boundary, demodulation and

#195241 - $15.00 USD Received 5 Aug 2013; revised 11 Sep 2013; accepted 18 Sep 2013; published 10 Oct 2013

unwrapping tasks (for each fringe-pattern) multiplies *N*-times possible error sources in 3D-shape profilometry [3–7]. Finally we need sum these real-valued, *N*-unwrapped phases coming from the *N*-perspectives [3–7]. In contrast co-phase profilometry "blindly" adds-up *N*-complex signals coming from frequency-shifting the set of *N*-fringe patterns. In conclusion, previous *N*-repetition of the whole profilometry processes applied to *N*-fringe-patterns [3–7], is reduced in co-phased profilometry to a single coherent phase-demodulation and a single unwrapping process of the whole set of *N*-fringe-patterns.

In this paper we propose to use a single-camera and *N*-projections directions illuminating the 3D-object. These *N*-fringe-projections minimize the shadows and specular reflecting zones from the 3D-object. After coherently summing *N*-analytical-signals, just a *single* unwrapping process is required..

2. Standard single-camera single-projector profilometry

The typical experimental set-up of single fringe-projection profilometry [1] is shown in Fig. 1.

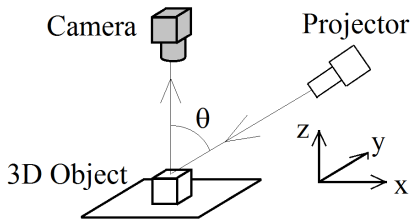

Fig. 1. Standard fringe projection profilometry with a single fringe-projection direction. The projector form a polar-angle θ with respect to the camera-object *z* axis.

The linear fringe-pattern projected towards the 3D object may be written as,

$$F(x,y) = 1 + \cos(v_0 x) \tag{1}$$

Where v_0 is the spatial frequency in radians per pixel. Assuming parallel illumination, the CCD camera sees the following phase-modulated fringe pattern [1] (see Fig. 1),

$$I(x,y) = a(x,y) + b(x,y)\cos\left[\omega_0 x + g\,O(x,y)\right];\ \ \omega_0 = v_0\cos(\theta),\ g = v_0\sin(\theta). \tag{2}$$

The function $a(x,y)$ is the background and $b(x,y)$ the contrast. The phase-modulated fringe-pattern in Eq. (2), has a spatial carrier $\omega_0 = v_0\cos(\theta)$, and sensitivity $g = v_0\sin(\theta)$ [1]; being θ the polar-angle. The contrast $b(x,y)$ has information about shadows and specular properties of the 3D object $O(x,y)$; it drops to zero $b(x,y) = 0$ at shadows and very-high reflections.

Fig. 2. In panel (a) we show the Fourier spectrum of the real-valued phase-modulated fringe pattern. In panel (b) we show the frequency-shifted spectrum and the low-pass filtering as a gray disk at the spectral origin.

The spatial (Fourier) phase-demodulation process is given by the following formula [1,2],

$$(1/2)b(x,y)e^{i g O(x,y)} = LPF\left[I(x,y)e^{-i\omega_0 x}\right]. \tag{3}$$

#195241 - $15.00 USD Received 5 Aug 2013; revised 11 Sep 2013; accepted 18 Sep 2013; published 10 Oct 2013

The operator $LPF[\bullet]$ is a low-pass filter (gray-disk in Fig. 2) which isolates the required object-phase information $gO(x,y)$ at the spectral origin [1,2,8,9].

3. Co-phased profilometry: Experimental set-up

For the sake of clarity assume a single camera and 4 collimated projectors at azimuthal phase-step angles $\varphi = \{0, \pi/2, \pi, 3\pi/2\}$, all having the same sensitivity polar-angle θ (see Fig. 3). Therefore the data consist of the following 4 phase-modulated fringe-patterns,

$$\begin{aligned} I_0(x,y) &= a_0(x,y) + b_0(x,y)\cos\left[gO(x,y) + \omega_0 x\right], \\ I_1(x,y) &= a_1(x,y) + b_1(x,y)\cos\left[gO(x,y) - \omega_0 x\right], \\ I_2(x,y) &= a_2(x,y) + b_2(x,y)\cos\left[gO(x,y) + \omega_0 y\right], \\ I_3(x,y) &= a_3(x,y) + b_3(x,y)\cos\left[gO(x,y) - \omega_0 y\right] \;;\; \omega_0 = v_0\cos(\theta),\, g = v_0\sin(\theta). \end{aligned} \tag{4}$$

Note that all $gO(x,y)$ remain invariant because the sensitivity polar-angle θ remains fixed.

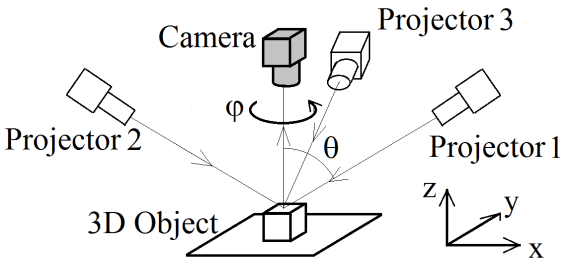

Fig. 3. Multiple projector co-phased profilometry experiment. Here a single camera and 3 projectors are shown. All projectors are at the same distance and have the same polar-angle θ.

The 4 projections have the same measuring sensitivity $g = v_0\sin(\theta)$ but different azimuthal angles φ. Note that all contrasts $b_n(x,y)$ are different due to the shadows and reflections from the 3D object $O(x,y)$ illuminated form 4 different azimuthal angles $\varphi = \{0, \pi/2, \pi, 3\pi/2\}$.

4. Spatial (Fourier) co-phased demodulation with 4-projector directions

Let us now coherently demodulate our 4-fringe-patterns in Eq. (4). This digital co-phased profilometry algorithm is a generalization of the standard Fourier method, and it is given by

$$A(x,y)e^{i\,gO(x,y)} = LPF\left[I_0(x,y)e^{-i\omega_0 x} + I_1(x,y)e^{i\omega_0 x} + I_2(x,y)e^{-i\omega_0 y} + I_3(x,y)e^{i\omega_0 y}\right]. \tag{5}$$

After low-pass filtering $LPF\{\bullet\}$ one obtains the following co-phased analytical sum,

$$A(x,y)e^{i\,gO(x,y)} = (1/2)\left[b_0(x,y) + b_1(x,y) + b_2(x,y) + b_3(x,y)\right]e^{i\,gO(x,y)}. \tag{6}$$

All these complex signals $b_n(x,y)e^{i\,gO(x,y)}$, $n = \{0,1,2,3\}$ are co-phased and added coherently. At places (x,y) where a given fringe-contrast is zero ($b_n(x,y) = 0$, due to shadows from $O(x,y)$); their sum $(1/2)\sum_n b_n(x,y) >> 0$ may still be much greater than zero, therefore obtaining a well-defined demodulated phase $gO(x,y)$.

#195241 - $15.00 USD Received 5 Aug 2013; revised 11 Sep 2013; accepted 18 Sep 2013; published 10 Oct 2013

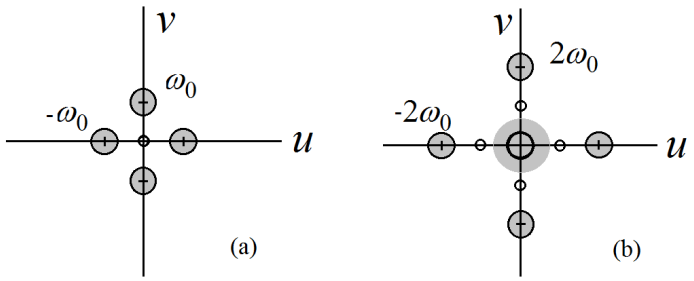

Fig. 4. Panel (a) shows the original Fourier spectra of the sum of 4 real-valued fringe patterns. In panel (b) we show the frequency shifted spectra of the sum in Eq. (5). At the spectral center in panel (b), the complex-spectrum of the 4 projected fringe-patterns adds coherently.

5. Co-phased profilometry with 4-projection perspectives and 3-temporal phase-steps

Of course we can use the Fourier phase demodulation procedure just seen. But phase-shifting profilometry is more accurate; so next we give some hints and an experiment on how to do it.

To avoid confusion, let us assume just 4-projection perspectives $\mathbf{d}_n = \cos(\varphi_n)\mathbf{i} + \sin(\varphi_n)\mathbf{j}$ at azimuthal angles $\varphi = \{0, \pi/2, \pi, 3\pi/2\}$, and 3-tempoaral phase-steps $\Delta = 2\pi/3$; totaling 4x3 = 12 spatial-temporal fringe-patterns,

$$I_n(x,y,m\Delta) = a_n(x,y) + b_n(x,y)\cos\{m\Delta + \omega_0 \mathbf{r}\bullet\mathbf{d}_n + g\,O(x,y)\},$$
$$with \quad \Delta = \frac{2\pi}{3}, \quad n \in \{0,1,2,3\}, \quad m \in \{0,1,2\}. \tag{7}$$

The vector $\mathbf{r} = x\mathbf{i}+y\mathbf{j}$ is the projector position. The co-phased demodulation algorithm is,

$$A(x,y)e^{i\,g\,O(x,y)} = IC_1 e^{-i\,\omega_0\,\mathbf{r}\bullet\mathbf{d}_0} + IC_2 e^{-i\,\omega_0\,\mathbf{r}\bullet\mathbf{d}_1} + IC_3 e^{-i\,\omega_0\,\mathbf{r}\bullet\mathbf{d}_2} + IC_4 e^{-i\,\omega_0\,\mathbf{r}\bullet\mathbf{d}_3}$$
$$IC_n(x,y) = I_n(0) + e^{-i\Delta} I_n(\Delta) + e^{-i\,2\Delta} I_n(2\Delta). \tag{8}$$

Some (x,y) were omitted for clarity. Of course this spatial-temporal algorithm may be generalized to N-projection perspectives $\{\mathbf{d}_0, \mathbf{d}_1, ..., \mathbf{d}_{N-1}\}$, and M-temporal steps $\Delta = 2\pi/M$.

6.- Experimental result with 2 projection perspectives and 4 temporal phase-steps

Here we present an experiment based on just 2-projections and 4-temporal phase-steps. Two projected fringes over the computer-mouse $O(x,y)$ are shown in Fig. 5. Our experimental data is formed by 2 projection-steps at azimuthal-angles $\varphi = \{0, \pi\}$, and 4-temporal phase-steps of $\Delta = 2\pi/4$; totaling 2x4 = 8 spatial-temporal phase-modulated fringe-patterns,

$$I_0(x,y,m\Delta) = a_0(x,y) + b_0(x,y)\cos\left[m\Delta + c_0(x,y) + gO(x,y)\right], \quad m = \{0,1,2,3\},$$
$$I_1(x,y,m\Delta) = a_1(x,y) + b_1(x,y)\cos\left[m\Delta + c_1(x,y) + gO(x,y)\right], \quad \Delta = \frac{2\pi}{4}. \tag{9}$$

The 8-spatial-temporal carriers are: $m\Delta + c_1(x,y)$ and $m\Delta + c_2(x,y)$ (see Fig. 5).

#195241 - $15.00 USD Received 5 Aug 2013; revised 11 Sep 2013; accepted 18 Sep 2013; published 10 Oct 2013

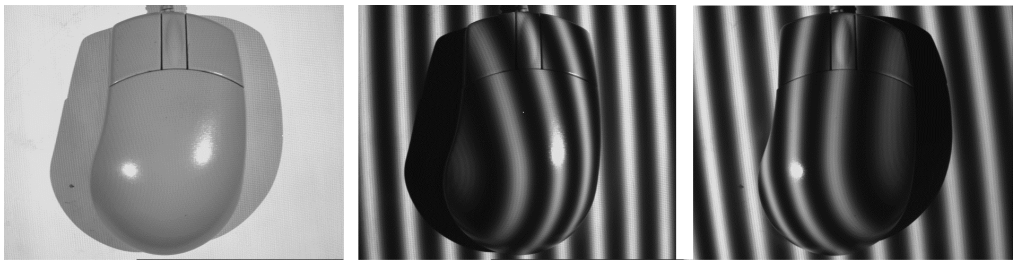

(a) (b) (c)

Fig. 5. In panel (a) we show the computer mouse illuminated with white light to see the object, the shadows and specular reflections from the two projector directions. Panel (b) and (c) show the projected fringes.

The projectors have divergent geometric distortion. Therefore the 2 spatial-carriers $c_1(x,y)$ and $c_2(x,y)$ must be estimated first by temporarily removing the object, *i.e.* $O(x,y)=0$) as,

$$\begin{aligned}(1/2)b_0(x,y)e^{ic_0(x,y)} &= I_0(0)+I_0(\Delta)e^{-i\Delta}+I_0(2\Delta)e^{-i2\Delta}+I_0(3\Delta)e^{-i3\Delta},\\ (1/2)b_1(x,y)e^{ic_1(x,y)} &= I_1(0)+I_1(\Delta)e^{-i\Delta}+I_1(2\Delta)e^{-i2\Delta}+I_1(3\Delta)e^{-i3\Delta}.\end{aligned} \tag{10}$$

Of course one may also use Fourier phase-demodulation to estimate $c_1(x,y)$ and $c_2(x,y)$, but with temporal phase-shifting interferometry one obtains a higher bandwidth estimation [9].

Once the spatial-carriers are estimated, the 3D-mouse is co-phased demodulated as,

$$\begin{aligned}A(x,y)e^{igO(x,y)} &= IC_0(x,y)e^{-ic_0(x,y)}+IC_1(x,y)e^{ic_1(x,y)},\\ IC_0(x,y) &= I_0(0)+I_0(\Delta)e^{-i\Delta}+I_0(2\Delta)e^{-i2\Delta}+I_0(3\Delta)e^{-i3\Delta},\\ IC_1(x,y) &= I_1(0)+I_1(\Delta)e^{-i\Delta}+I_1(2\Delta)e^{-i2\Delta}+I_1(3\Delta)e^{-i3\Delta}.\end{aligned} \tag{11}$$

The co-phased profilometry of this computer mouse is shown in Fig. 6.

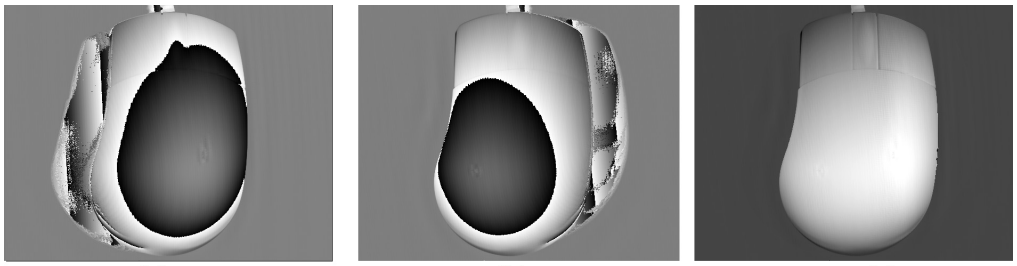

(a) (b) (c)

Fig. 6. Panel (a) shows the 4-temporal-steps demodulated-phase from the right projection. Panel (b) shows the 4-temporal-steps demodulated-phase from the left projection. Panel (c) shows (already unwrapped) the phase of the coherent-sum of both analytical signals, and we see that the phase-object is recovered without errors due to the shadows and specular bright zones.

In Figs. 6(a) and 6(b) one can see the shadow phase-noise regions where the contrast of the right and left projections drops, $b_0(x,y)=0$, and $b_1(x,y)=0$. Finally Fig. 6(c) shows the unwrapped mouse-phase $gO(x,y)$ from our co-phased demodulation algorithm. Figure 6(c) shows the whole mouse without the shadow-noise seen in the two individual projected fringe-patterns in Figs. 5(b), 5(c) (Figs. 6(a), 6(b)). Finally due to the low phase-noise in digital profilometry we used simple line-integration phase-unwrapping to obtain Fig. 6(c).

#195241 - $15.00 USD Received 5 Aug 2013; revised 11 Sep 2013; accepted 18 Sep 2013; published 10 Oct 2013

7. Alternative experimental set-up for co-phase profilometry

Here we give another (we think) more robust, co-phased experimental set-up.

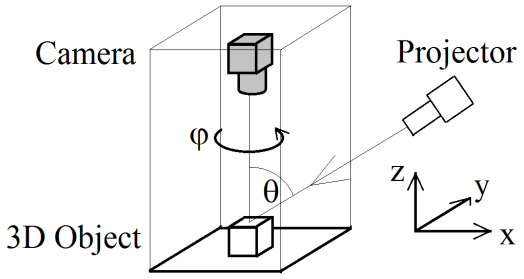

Fig. 7. Single-projector, single-camera, multiple projections co-phased profilometry set-up. Here the camera-object system is rotated as a rigid square-box an azimuth-angle φ, around z. In this way one obtains as many 3D object's perspective steps as desired. All other relative distances and angles (including the sensitivity polar-angle θ) remain fixed.

Using the set-up in Fig. 7 one avoids the easy-but-tedious-task of matching all the experimental projector's distances within millimeter tolerances. In any case, no optical-wavelength tolerances as in co-phasing large segmented telescopes are required.

8. Demodulated phase-noise considerations in co-phase profilometry

Let us rewrite Eq. (6) assuming phase-additive, statistically-independent measuring-noise,

$$A(x,y)e^{igO(x,y)} = (1/2)\left[b_0 e^{in_1(x,y)} + b_1 e^{in_2(x,y)} + b_2 e^{in_3(x,y)} + b_3 e^{in_4(x,y)}\right] e^{igO(x,y)}. \quad (12)$$

All these phase-noise $\{n_1(x,y), n_2(x,y), n_3(x,y), n_4(x,y)\}$ are independent, so this is the same case (from the phase-noise perspective) as having 4-temporal phase-steps in a single-projector ($b_0(x,y)$) configuration. In this later case one would obtain,

$$A(x,y)e^{igO(x,y)} = (1/2)\left[b_0 e^{in_1(x,y)} + b_0 e^{in_2(x,y)} + b_0 e^{in_3(x,y)} + b_0 e^{in_4(x,y)}\right] e^{igO(x,y)}. \quad (13)$$

At places with good fringes $b_n(x,y) >> 0$ (in Eq. (12)), the demodulated phase-noise power is reduced by 4 (four) [8,9]. In Eq. (13) we have single-projection and 4 temporal phase-steps $\Delta = \{0, \pi/2, \pi, 3\pi/2\}$, while in Eq. (12) we have 4-projections at azimuthal phase-steps $\varphi = \{0, \pi/2, \pi, 3\pi/2\}$. Therefore Eq. (12) and Eq. (13) are equally noisy at places with no shadows or high reflections, *i.e.* $b_n(x,y) >> 0$.

9. Conclusions

Here we have presented a single-camera, *N*-projections co-phased profilometry technique for shape measurement of 3D objects. The set of digitized *N*-fringe-patterns is coherently demodulated in a single phase-estimation process. The single-step co-phased demodulation of *N*-fringe-patterns taken from *N*-perspectives minimizes the shadows and specular reflections from the 3D object being digitized. We have presented 2 alternative experimental set-ups, both easily implemented within millimeter tolerances. We have carried out a simple profilometry experiment based on 2-projection perspectives combined with 4-temporal phase-steps. Using 2 projection directions we were capable of eliminating the shadows and specular reflections from a computer-mouse under analysis. Co-phasing *N*-fringe-patterns is mathematically similar to co-phasing *N*-mirrors in a large segmented telescope.

#195241 - $15.00 USD Received 5 Aug 2013; revised 11 Sep 2013; accepted 18 Sep 2013; published 10 Oct 2013